Probing the mechanism by which ceramic dispersants act

A. U. Khan, P. F. Luckham and S. Manimaaran

Department of Chemical Engineering, Imperial College of Science, Technology and Medicine, Prince Consort Road, London, UK SW7 2BY

Herein is described our efforts to better understand the mechanisms that control the interactions between stabilised ceramic powders. To this end we have employed two distinct experimental techniques, rheology and atomic force microscopy (AFM). The two techniques have been used in conjunction here for the specific task of examining the effects of Darvan C, a polyelectrolyte on the dispersability of an alumina powder. The AFM technique enables one to obtain information concerning the interaction between alumina particles. The results showed that at a pH of 6.0 the interactions between alumina particles are attractive, but in the presence of Darvan C the interactions are repulsive. This gives rise to a suspension of alumina particles having a markedly lower viscosity in the presence of Darvan C. Similar effects were also found at pH values away from the isoelectric point of the alumina, where there is also a repulsive interaction between the particles.

Quality ceramic processing requires favourable system interactions so as to minimise cost and maximise ease of manufacture.[1] In the absence of dispersants or deflocculants such a condition is not easily achieved, as the attractive forces present between particles can lead to flocculation when introduced into solution.[2] Stability can however be imparted by way of steric or electrostatic effects, and their success at doing so has traditionally been investigated at a macroscopic level using well established methods such as rheology.[3–5] Although the success of these studies are beyond question they do have one shortcoming—they do not provide us with a definitive view describing the interactions at a particulate level. The work presented here attempts to address this point by investigating the nature of the interactions between particles, by making use of a relatively new tool, atomic force microscopy (AFM).[6] AFM is currently the best tool available allowing us to mimic the interactions that may occur between two particles.[7–10]

In this study, Darvan C, a polyelectrolyte, has been investigated under a variety of conditions so as to gain a more complete understanding of the interactions that take place in systems stabilised by it. Rheological data retrieved from a Bohlin rheometer are compared with data obtained at a nanoscale using a Topometrix Explorer AFM.

Experimental

Materials

Alumina AES-11 (Mandoval Ltd., Surrey, UK) was used in the present study. Alumina AES-11 was 99.8% pure, had a BET surface area of 8.14 m^2 g^{-1} and a mean particle size of 0.4 μm.

The dispersant, Darvan C (R. T. Vanderbilt Company Inc., USA) is available in the form of an aqueous solution (25% active component). Darvan C is a polyammonium methacrylate material, and its structure is shown in Fig. 1.

For the atomic force microscopy experiments a sapphire (alumina) surface, obtained from Goodfellow Metals Plc., Cambridge, was used.

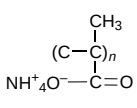

Darvan C

Fig. 1 Chemical structure of the dispersant Darvan C

Sample preparation

Submicrometer powder materials such as alumina form agglomerates upon storage. These agglomerates may be weak or strong depending upon the forces acting between the particles. In order to prepare homogeneous suspensions, which is essential to obtain a high-quality product, the agglomerates must be broken up into primary particles. There are several ways to achieve this goal. Common to all of these is the supply of energy which can overcome the attractive forces between the particles. The most common method is to apply mechanical agitation which is usually applied when the powder is wet and de-aired. The methods used to prepare samples for this were ball milling and ultrasonication.

The following procedure was adopted for all the ball milling operations: spherical balls of alumina (diameter 0.5–1.5 mm) were placed into a 500 or 250 ml (depending on the amount of suspension to be prepared) high-density poly(ethylene) bottle. The total volume of the balls was such they were just submerged in the constituents of the suspension. A given volume of water was then added followed by a measured amount of the dispersant (if required) in the form of solution. A known mass of the powder was then added and the sample was ball milled for a fixed time period at a specific rotational speed.

Ultrasonication

Before ultrasonication the sample containers were placed in ice-cold water to prevent warming of the sample. In preparing the suspensions the following procedure was adopted. A given volume of water was added to the container/bottle and the required amount of dispersant, in the form of solution, was added and shaken gently. The powder was then added to the sample container and the sample was ultrasonicated for a fixed time.

The ultrasonicator used was a Vibra-Cell VCX-600 (Sonic and Materials, Connecticut, USA) which has a vibrational output of 20 kHz and a maximum power output of 600 W. The equipment operated between 60 and 70% of the maximum output and the time of ultrasonication was changed according to the quantity of the suspension. The control/display unit of the ultrasonic probe also displays on-line the power consumed by the unit to disperse the particles. This power consumption also indicates indirectly the quality of the dispersion. At the early stages, when the particles are agglomerated and not adequately dispersed, the power display unit indicates a

comparatively high output consumption which gradually decreases and becomes virtually constant. At this constant value it may be considered that all the agglomerates have been broken up.

Adsorption isotherms

A stock solution which corresponds to a Darvan C concentration of 4% dmb (dry mass basis of the powder) was prepared, and then diluted to 40 ml aliquots of known concentration. Using *ca.* 15 ml of these aliquots, eight or so suspensions containing *ca.* 5 g powder were prepared. All the dispersions were first ultrasonicated and then equilibrated for 48 h in a tumbler agitator. The particles were separated by using an MSE 25 centrifuge at 13000 rpm for 6 h and the clear supernatant was removed.

A UV–VIS spectrophotometer (Perkin Elmer 554) was used to measure the concentration of the supernatant resulting from the separation of the particles. To measure the adsorbed amount of the dispersant, a calibration curve was constructed at a wavelength of 232 nm. From the calibration curves, the difference in concentration before and after adsorption was determined, and hence the amount adsorbed calculated.

Electrophoretic mobility measurements

Stock suspensions containing *ca.* 1% (m/v) particles with and without dispersant were prepared in a 10^{-3} M KNO_3 solution. The suspensions were ultrasonicated by using a Vibra-Cell VCX 600 ultrasonicator. A few drops of the stock suspension were used to prepare several more diluted suspensions (30 ml in volume) in a known KNO_3 electrolyte concentration (10^{-3} M). The pH of the suspensions was adjusted and the samples stored overnight. Prior to the electrophoresis experiments the pH of the suspensions was measured.

The electrophoretic mobility of the particles was determined with a Zeta Master microelectrophoresis instrument (version PCS, Malvern Instruments, UK). The average mobility was then calculated from the average of at least 15 different experimental runs.

Rheology

All rheological measurements were performed on a Bohlin VOR rheometer (Bohlin Reologi, Lund, Sweden), interfaced with a computer. The instrument can operate in both continuous shear and oscillatory shear mode. A concentric cylinder C25 measuring system was used.

In the steady shear rate mode of the Bohlin instrument, the outer cylinder of the rheometer is rotated at known shear rates, $\dot{\gamma}$. The resulting stress, σ, in the sample is transmitted to the inner cylinder, whose movement is then measured by a transducer connected to the inner cylinder by an interchangeable torque bar (covering a wide range of sensitivities.) Hence, the apparent viscosity, η, is measured as a function of shear rate:

$$\eta = \sigma/\dot{\gamma} \quad (1)$$

The alumina suspension was placed into the measuring cylinder *via* a pipette or spatula, and a solvent trap was placed over the entire geometry, sealing the system to minimise changes in volume fraction by evaporation of water. The sample was sheared at a very high shear rate of *ca.* 960 s^{-1} and then allowed to equilibrate for at least two min before measurements were started. The viscosity at low shear rates was measured first, stepping up to higher shear rates, and then back to low shear rates, covering the shear rate range 10^{-1}–10^{3} s^{-1}. All experiments were performed at 25 °C.

In oscillatory shear experiments, a small amplitude sinusoidal strain (or stress) with frequency ν/Hz is applied to the system and the stress and strain compared simultaneously. The maximum amplitude of the stress is τ_o and oscillates at the same frequency as the strain. For a perfectly elastic solid, the stress is exactly in phase with the strain, whereas for a perfectly viscous liquid, it is 90° out of phase with the strain. For a viscoelastic material the phase angle shift δ lies between 0 and 90°.

Thus, by measuring the maximum strain γ_o and stress τ_o amplitudes and the phase angle shift one can characterise the viscoelastic properties of the system. These are defined by three main parameters: the complex modulus, G^*, the storage modulus, G', and the loss modulus, G'', with:

$$G^* = \tau_o/\gamma_o \quad (2)$$

$$G' = G^* \cos\delta \quad (3)$$

$$G'' = G^* \sin\delta \quad (4)$$

G' is the elastic component of the complex modulus G^*, which is a measure of the energy stored during a cycle of deformation. G'' is the viscous component of the complex modulus and is a measure of the energy dissipated (as heat) during a cycle of deformation.

Initially, strain sweep measurements were performed in which the strain amplitude γ_o was varied while the frequency was kept constant (usually 1 Hz). G^*, G' and G'' were measured as a function of γ_o in order to obtain the linear viscoelastic region. The values of G^*, G' and G'' remained constant with increasing γ_o until a critical strain γ_{cr} was reached where G^* and G' began to decrease whilst G'' increases. The region where G^*, G' and G'' are independent of the applied strain amplitude is referred to as the linear viscoelastic region. Once the linear viscoelastic region was established, measurements were carried out either as a function of frequency or temperature at constant strain (choosing an amplitude within this region).

Atomic force microscopy

Atomic force microscopy (AFM) has in recent years become a standard technique for the imaging of surface topographies in both industry and academia. However until recently the use of the AFM as a force sensing tool has been limited. The apparatus used here was a Topometrix explorer atomic force microscope which was used in the 'force spectroscopy' mode.

In atomic force microscopy, a small soft cantilever is used to sense the forces at an interface. The lever–surface separation is controlled by a piezoelectric ceramic to nanometer resolution, and the deflection is determined using optical beam deflection. Beam deflection is intrinsically vibration tolerant (due to its inherent gain) and is relatively immune to contaminants and the media used, compared to other techniques. The beam deflection was monitored by a split, four-quadrant, position-sensitive detector (PSD). This allowed both the vertical and lateral spot motions to be resolved (*i.e.* the twisting as well as the bending of the lever). Data were captured using the standard Topometrix software, but all processing thereafter was done off-line on commercial spreadsheet software. The force resolution of the set-up was of the order of 100 pN. The AFM lever is driven towards the surface by a piezoceramic at a rate of 1–10 nm s^{-1}. In this way force distance profiles between the AFM tip and surface can be determined. In this study a commercial silicon nitride AFM tip with a tip radius of *ca.* 50 nm and a spring constant of 0.3 N m^{-1} was used, and a flat sapphire (alumina) disk was used as the lower, binding surface. Even though this is an asymmetric set-up it is appropriate in the case of this study as a result of silicon nitrides 'immunity' to Darvan C adsorption under the experimental conditions employed. It has been verified by other workers that silicon nitride particles aggregate in water at neutral pH. Furthermore, they are not dispersed after the addition of Darvan C, *i.e.* Darvan C does not stabilise silicon nitride particles in water. However, Darvan C is well estab-

lished as a dispersant for alumina particles, and as we are concerned here with establishing the mode of stabilisation in the particular case of sapphire particles, it is quite appropriate to use a 'neutral' probe (the silicon nitride tip).

Prior to each experiment, the lower sapphire surface was cleaned in a surfactant solution followed by rinsing and further thorough cleaning in nanopure water so as to ensure the removal of any active agents on the surface. An ultrasonic bath was employed for the cleaning procedure. More often than not, a new tip was used for each experiment. However, when it was necessary to clean the tip, it was considered sufficient to rinse the tip repeatedly. The ultrasonic bath was not employed to clean the tip as it was feared that such a procedure would damage it. After cleaning, the surfaces were then allowed to dry overnight in a laminar flow hood in a class 1000 clean room. The cleaned surfaces were then mounted on the AFM, and nanopure water injected in between the surfaces. This procedure was adopted as a matter of routine, as the results of the water experiment could be used to ascertain the cleanliness and therefore the suitability of the two surfaces for further experimentation. Appropriate reproducible results at a number of sites on the sapphire surface were used as guidelines for further experimentation involving the surfaces in question.

Once satisfactory profiles were obtained in water, the water was drained away from the gap, and a solution of the dispersant being investigated was injected in between the surfaces. After allowing the system to equilibrate for *ca.* 1 h, force measurements were then carried out on the system at a number of sites. Once again, reproducible results at a number of sites were seen to indicate the validity of the results.

Results and Discussion

Fig. 2 shows the adsorption isotherm for Darvan C on alumina AES-11. The adsorption is of a high affinity type, typical of polyelectrolyte adsorption to surfaces.

Fig. 3 shows the electrophoretic mobility of the alumina samples plotted as a function of pH with 1% Darvan C and without any dispersant. In the absence of Darvan C the isoelectric point is at pH *ca.* 7.5, which is typical for alumina suspensions. It is clear that the Darvan C has shifted the isoelectric point (i.e.p.) to pH *ca.* 4.0. When Darvan C is adsorbed on the surface of the particles, the hydroxy groups of the titrant will react with the carboxylic groups of Darvan C and this will result in a shift of the i.e.p. to a lower value.

Fig. 4 shows the viscosity of a suspension of 40% (by volume) alumina, as a function of Darvan C concentration at three different shear rates. At all shear rates for low concentrations of dispersant, the viscosity is reduced as the concentration of Darvan C is increased. The dynamic rheological results of the alumina suspension, 40% (v/v) suspension against the Darvan C concentration at a frequency of 1 Hz are shown in Fig. 5. The parameters, G^*, G' and G'' show the same trend as seen in the shear viscosity data at different shear rates. The values of all the moduli decrease as the Darvan C concentration is increased from 0.25% to 1% dmb. They then increase gradually as the Darvan C concentration is increased beyond 1 to 4% dmb. This reduction of the viscosity and moduli is a result of the aggregates in the suspension breaking down into smaller flow units. It is clear from the above figures that a concentration of Darvan C of *ca.* 1% dmb gives the lowest

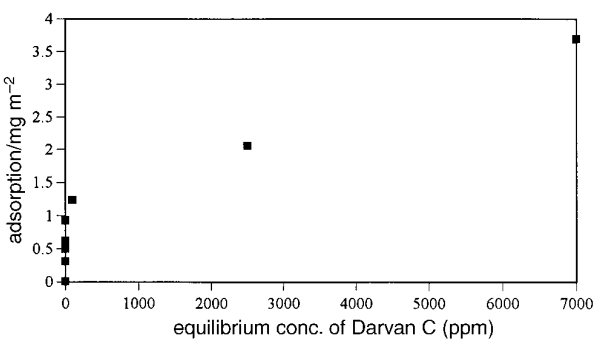

Fig. 2 Adsorption isotherm for the adsorption of Darvan C to alumina at pH 6.0 and 25 °C

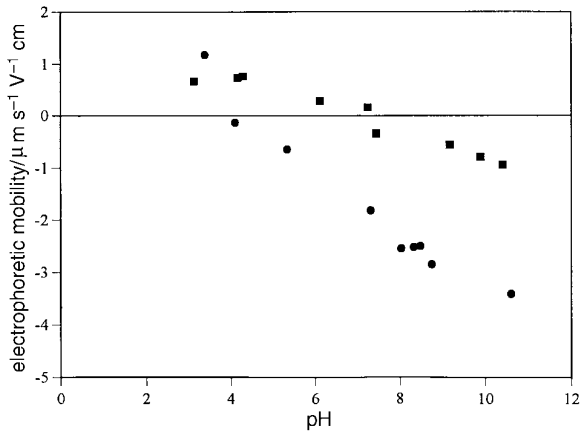

Fig. 3 Electrophoretic mobility of alumina as a function of pH, with (■) and without (●) Darvan C

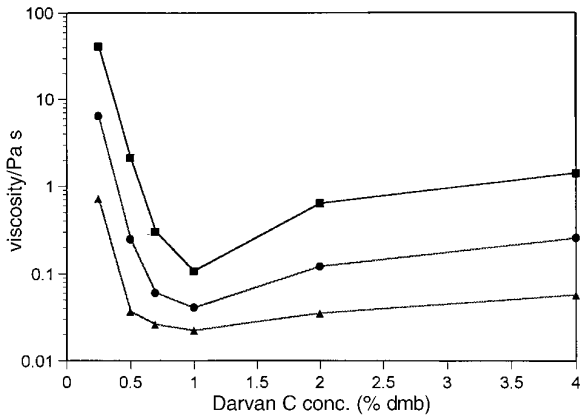

Fig. 4 The viscosity of alumina 40% (v/v) suspensions as a function of Darvan C concentration at three different shear rates: ■, 1.46 s^{-1}; ●, 14.6 s^{-1}; ▲, 146 s^{-1}

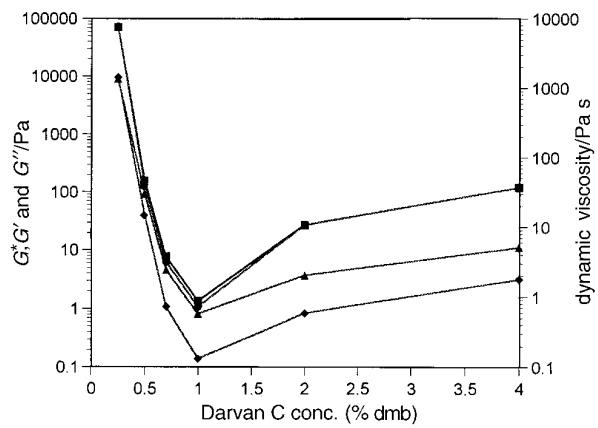

Fig. 5 G^* (■), G' (●), G'' (▲) and the dynamic viscosity (◆) of alumina 40% (v/v) suspensions as a function of the Darvan C concnetration at a frequency of 1 Hz

viscosities and moduli. A 1% dmb concentration of the dispersant corresponds to a surface coverage of 1.23 mg m^{-2} of Darvan C (or 0.31 g m^{-2} active component). When the concentration of Darvan C is $<1\%$, the surface coverage of the particles is incomplete and the particles flocculate owing to van der Waals attraction. The adsorption isotherm (Fig. 2) also shows that when the amount of Darvan C is $<1\%$ dmb there is insufficient dispersant to completely cover the surface of the particles.

From the adsorption isotherms it can be seen that the concentration of dispersant that gives the lowest viscosity and other viscoelastic parameters corresponds to virtually all the dispersant being adsorbed on the particles and that the equilibrium concentration is negligible. Thus the rheology data suggest that as the dispersant is added the attractive interactions between the particles is reduced and eventually the interactions become repulsive. AFM force profiles, where the interaction can in principal be measured directly, should confirm this hypothesis.

Fig. 6 shows the force–distance profile for the interaction between an AFM tip and a sapphire surface in nanopure water at pH 6.0. The profile shows an attraction at *ca.* 50 nm due to the van der Waals attractive forces between the surfaces. On separation the surfaces remain in contact owing to the strong attractive forces present between the two surfaces, until they spring apart by some 200 nm or so. We conclude that in a suspension prepared by dispersing an (alumina) powder in water, *i.e.* such that the initial state of the particles is aggregated, the particles will remain in an aggregated state and have a relatively high viscosity.

Fig. 7 shows a force–distance profile taken *ca.* 1 h after the addition of the dispersant Darvan C. In this profile a short-range repulsion commencing at surface separations of some 35 nm is observed and there are no apparent attractive interactions between the two surfaces. Hence we would conclude that under these conditions the alumina particles are repelling each other in a suspension and that the viscosity would be low. Although this confirms the expected result of Darvan C acting as a dispersant for alumina particles, it does not provide us with a clear explanation for the mode of stabilisation, *i.e.* whether the stabilisation is due to steric interactions between the adsorbed Darvan C layers or to electrostatic interactions, due to an increase in the surface charge, or a combination of both factors.

Fig. 8 shows the results obtained from a buffered solution of nanopure water at pH 3. This shows a short(er) range attraction (setting in at *ca.* 10 nm), followed by an even shorter range repulsion possibly due to electrostatic effects (illustrated by the curvature of the profile prior to hard contact, *cf.* pH 6 which shows a hard-wall repulsion). At pH 3 it can be safely assumed that both surfaces will carry a positive charge, and this is responsible for the observed long-range repulsion, with van der Waals forces being dominant at shorter separations.

Fig. 9 shows results obtained from a solution of Darvan C at pH 3. It is important to recognise that at this pH, Darvan C carries virtually no charge. This profile once again shows the attractive force present in the absence of Darvan C, is replaced by a repulsion, but one that is significantly shorter range than at pH 6 (Fig. 7). As Darvan C is uncharged at this pH, and the surfaces have a clear attractive force profile in its absence, it can be concluded that Darvan C must be stabilising the system sterically, *i.e.* Darvan C must be physically adsorbed onto the sapphire surface, and the extension of the Darvan C molecules in to the solution provides a steric barrier that physically prevents the close approach of the surfaces. This implies that the profile obtained at the higher pH, Fig. 7, which shows a noticeably longer range repulsion, may well be due to a combination of steric and electrostatic effects.

Fig. 10 shows the results for both nanopure water and Darvan C at pH 9 and indicates a repulsive interaction of similar range for both nanopure water and the Darvan C solution, implying that the interaction is largely electrostatic in both cases.

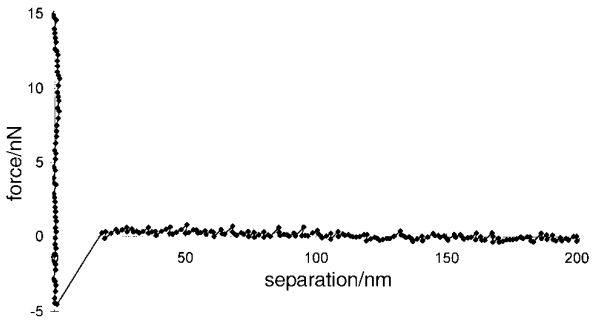

Fig. 6 Interaction between a sapphire surface and a silicon nitride AFM tip of radius 50 nm in water at pH 6.0 in the absence of any added Darvan C

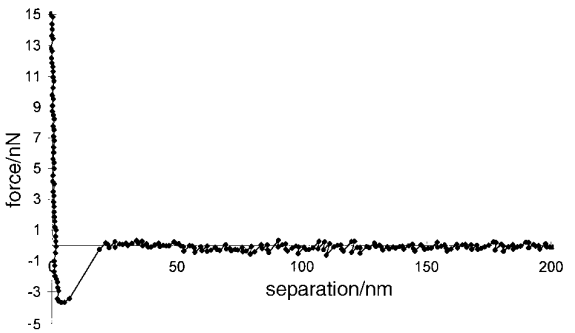

Fig. 8 Interaction between a sapphire surface and a silicon nitride AFM tip of radius 50 nm in water at pH 3.0 in the absence of any added Darvan C

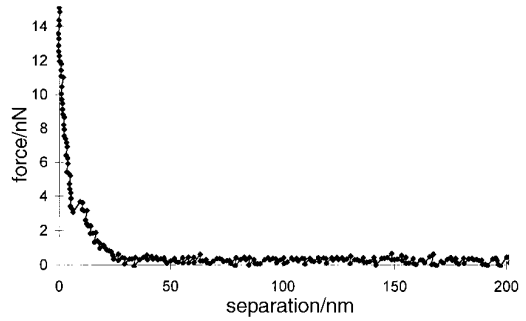

Fig. 7 Interaction between a sapphire surface and a silicon nitride AFM tip of radius 50 nm in water at pH 6.0 in the presence of a 1% solution of Darvan C

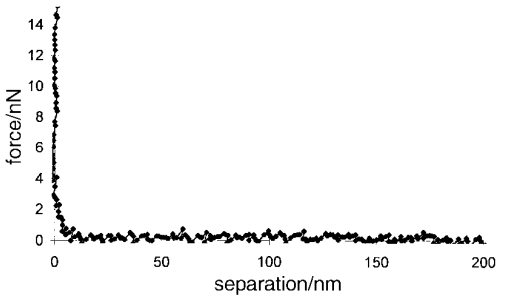

Fig. 9 Interaction between a sapphire surface and a silicon nitride AFM tip of radius 50 nm in water at pH 3.0 in the presence of a 1% solution of Darvan C

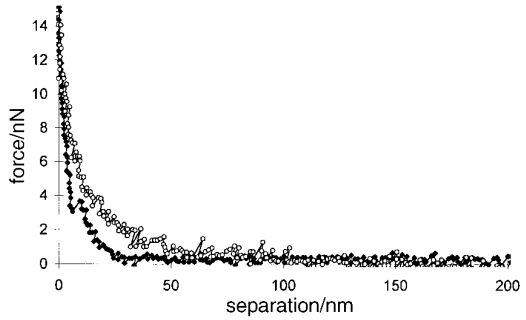

Fig. 10 Interaction between a sapphire surface and a silicon nitride AFM tip of radius 50 nm in water at pH 9.0 with (○), and without (●), a 1% solution of Darvan C

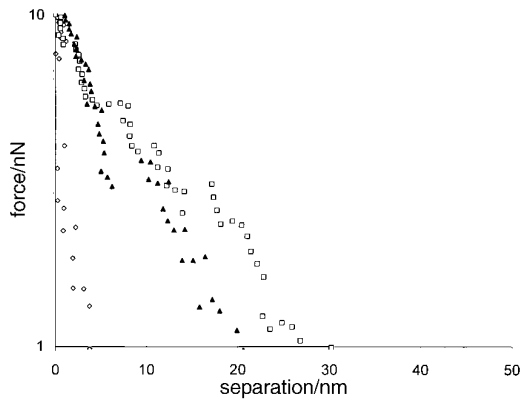

Fig. 11 A semilogarithmic plot of the interactions between Darvan C coated alumina surfaces at pH 3.0 (◇), pH 6.0 (▲) and pH 9.0 (□)

Finally, Fig. 11 presents a semilog plot of the interaction profile for Darvan C at a variety of pH values. They show a linear relation at pH 6 and 9, implying that the interaction is largely electrostatic in nature but at pH 3, where the Darvan C dispersant is uncharged, the polymer must be acting as a steric stabiliser. The lack of any attractive interaction in the presence of Darvan C means that the van der Waals attractive forces have been overcome by a repulsive interaction. It is not possible for electrical double layer repulsion to achieve this. Thus, at short range there must also be a steric repulsive interaction between the two surfaces. This leads us to the conclusion that Darvan C acts as an electrosteric dispersant for alumina particles. At long range the interaction between the coated alumina surfaces (particles), is due principally to double layer overlap, whilst at short range a steric mechanism is also acting which prevents the surfaces adhering (and hence the particles coagulating).

Conclusions

To conclude, we can state from our data that when the interactions between ceramic particles are repulsive, a minimum in the rheological properties, such as viscosity, is observed. Since it is under these conditions of minimum viscosity that ceramics are frequently processed these results have clear implications in the processing of ceramics. At low and high pH the interactions between the particles are inherently repulsive, so the effect of adding a dispersant may be limited. However, at pH 7, the addition of a dispersant, Darvan C, induces a repulsive interaction between the particles in a ceramic dispersion. In our opinion this is probably due to a combination of electrical double layer and steric interactions.

We would like to thank the EPSRC, the European HCM grant number CHRX CT94 0574 and the Pakistan Government for their financial support of this work.

References

1 D. W. Richerson, *Modern Ceramic Engineering*, Marcel Dekker, New York, 1982, pp. 147–300.
2 Th. F. Tadros, in *Solid/Liquid Dispersions*, ed. Th. F. Tadros, Academic Press, London, 1987, pp. 1–16, 225–274, 293–327.
3 W. Liang, Th. F. Tadros and P. F. Luckham, *J. Colloid Interface Sci.*, 1992, **153**, 131.
4 B. J. Briscoe, A. U. Khan, P. F. Luckham and N. Ozkan, in *Fourth Euro-ceramics*, ed. C. Galassi, Gruppo Editoriale Faenza Editrice S.p.A, Italy, 1995, vol. 2, pp. 93–100.
5 S. Biggs, P. J. Scales, Y. K. Leong and T. W. Healy, *J. Chem. Soc., Faraday Trans.*, 1995, **91**, 2921.
6 G. Binnig, C. F. Quate and Ch. Gerber, *Phys. Rev. Lett.*, 1986, **56**, 930.
7 W. A. Ducker, T. J. Senden and R. M. Pashley, *Nature* (*London*), 1991, **353**, 239.
8 S. Biggs and T. W. Healy, *J. Chem. Soc., Faraday Trans.*, 1994, **90**, 3415.
9 S. Biggs, *Langmuir*, 1995, **11**, 156.
10 G. J. C. Braithwaite, A. Howe and P. F. Luckham, *Langmuir*, 1996, **12**, 4224.

Paper 7/01170I; *Received* 19*th February*, 1997